Integration of MEMS Inertial Sensor-Based GNC of a UAV

Z. J. Huang and J. C. Fang

School of Instrumentation & Optoelectronics Engineering,
Beihang University, Beijing 100083, China

huangzhongjun@buaa.edu.cn, fangjiancheng@buaa.edu.cn

Abstract

Applying Micro Electromechanical Systems (MEMS) inertial sensors for the Guidance, Navigation and Control (GNC) of an autonomous Unmanned Aerial Vehicle (UAV) is an extremely challenging area. This paper presents a practical approach of applying an Inertial Navigation System (INS) using MEMS inertial sensors, Global Positioning System (GPS) receiver, Magnetometer and Barometer for the GNC. The focus of this paper is the design of a 250-g Micro-GNC for autonomous UAV. The INS/GPS/Mag/Baro integrated navigation loop provides continuous and reliable navigation solutions to the guidance and flight control loop. The guidance loop computes the guidance demands from the current UAV states to satisfy mission requirements. The flight control loop generates actuator control signals to transports the UAV to the desired location. The whole GNC algorithm was implemented within an embedded flight control computer. The real-time flight test results show that the UAV can perform the autonomous flight reliably.

Keyword: IMU, INS, GPS, UAV, MEMS, Navigation, Integrated System.

I. Introduction

Over the recent years, Unmanned Aerial Vehicle (UAV) has been designed for applications as fire monitoring, agriculture, mining, search and rescue. In order to become successful, the cost of these systems has to be affordable. Thus researching on the Guidance, Navigation and Control (GNC) of a UAV using Micro Electromechanical Systems (MEMS) sensors is important. However, when applying MEMS inertial sensors, the stability of the Inertial Navigation System (INS) will be degraded by the MEMS inertial sensor drifts. The quality and integrity of aiding sensors becomes more crucial for the integrated system[1].

The Global Positioning System (GPS) can provide long-term stability with high accuracy and worldwide coverage. Since the performance of the low cost micro GPS receiver can be easily degraded in high maneuvering environments, fusing the navigation data with other sensors such as a magnetometer or barometer is necessary.

So far, there are a broad of research on the design, fabrication and testing of MEMS inertial sensors[2,3,4,5,6], the integration and alignment of MEMS sensor-based inertial measurements unit (IMU)[7,8], the algorithm of MEMS sensor-based inertial navigation system (INS), the integration and algorithm of GPS/INS integrated system[9,10,11] and the GPS/INS/Mega integrated system[12].

This paper present a MEMS sensor-based micro GNC system which is successfully applied to a UAV, as shown in fig. 1. The physical UAV system comprises of the flight platform, onboard systems, communication links, and ground station. The UAV states are downlinked to the ground station for UAV state monitoring. There are two flight control modes. In remote operation mode, the pilot on the ground sends the control signals to the actuator via wireless uplink channel. In autonomous mode, the navigation output is fed into the guidance and control loop and the onboard Flight Mode Switch redirects the computed control outputs to the actuators. The whole GNC algorithm was implemented within an embedded flight control computer ARM9. The UAV is a fixed wing platform with a pusher prop configuration. It carries an extra CMOS vision sensor. The real-time flight tests show that the navigation system can provide accurate and reliable 3D navigation solutions as well as to perform the guidance and control task reliable.

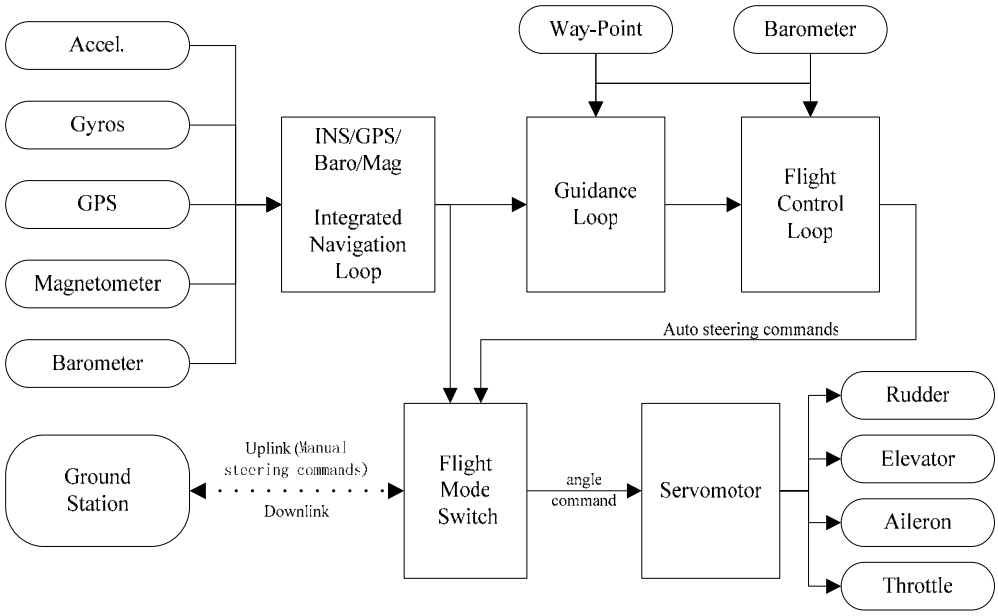

Fig. 1. The structure of MEMS sensor based micro GNC

II. Aircraft System

To meet the need of remote distance flight mission, the flight platform is designed as a delta fixed wing platform with an electromotor pusher prop configuration, as shown in fig. 2. It is capable of flying at 21m/s and up to 500m. The platform can carry up to 2kg of additional mission payload. Table 1 shows the specifications for the flight platform. The aerofoil is S7055. In this case, the lift/drag ratio has the maximum of 70. The lift coefficient is limited to 1.1 based on the aerofoil data. The minimum velocity can be written as

$$V_{\min} = \sqrt{\frac{2W}{\rho S C_{L\max}}} \approx 12m/s \quad (1)$$

Where S is the wing area and $C_{L\max}$ is the maximum lift coefficient.

Fig. 2. The flight platform structure

Table 1. Flight platform specifications

Wingspan	2.8m
Wind area	0.87m^2
Wing loading	103g/dm^2
Max. takeoff weight	9kg
Payload	2kg
Flight time	30min
Max. speed	25m/s
Min. speed	12m/s

Fig. 3 shows the wind tunnel test, where the flight platform model is reduced to 1/5 in size. Fig. 4 shows the lift coefficient, drag coefficient and lift/drag versus the platform angle of attack respectively.

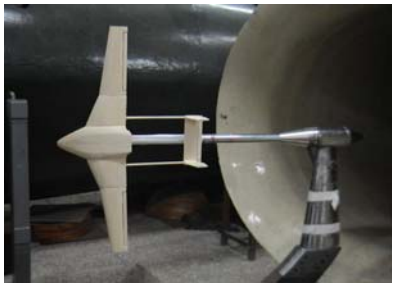

Fig. 3. wind tunnel test

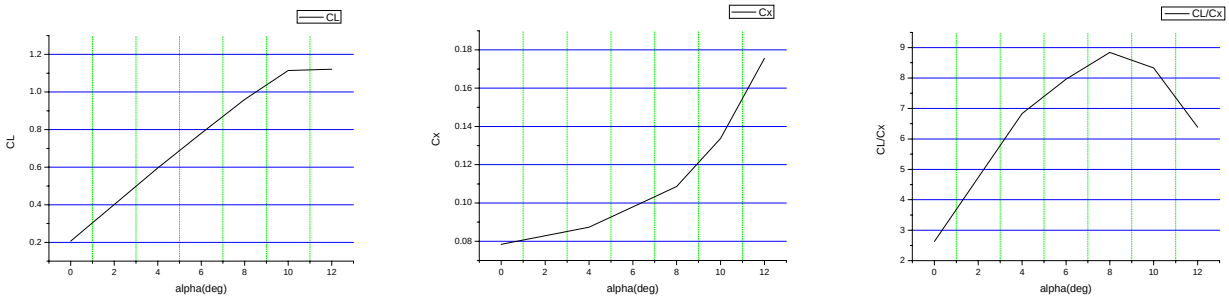

Fig. 4. Lift coefficient, drag coefficient and lift/drag versus the platform angle of attack respectively

The onboard systems consist of a GNC system, vision system and a 900MHz wireless data link. The vision system is mission payload for target tracking, target registration and decentralized data fusion.

The air-to-ground communication links are used for the UAV monitoring, remote control operation, and telemetry data. The ground station is a monitoring computer.

III. Sensors

MEMS inertial sensors are of utmost important in the GNC system. Processed by using Silicon-On-Insulator (SOI) techniques, The MEMS inertial sensors structure has the advantages of low stress and high aspect-ratio. Fig. 5 shows the MEMS gyros and its microstructure. Fig. 6 shows the measured output signal versus input angular rate. The output voltage is proportional to the input angular rate and changed linearly in the range -500 to 500°/s. The gyro bias repeatability is 0.01°/s.

Fig. 7 shows the accelerometer and its microstructure. The accelerometer has a bias repeatability within 1 mg. The MEMS Inertial Measurement Unit (IMU) is a six-degree of freedom inertial measurement unit consisting of three orthogonal MEMS accelerometers and gyros. The accelerometers and gyros are mounted in body coordinates and are not mechanically moved. These sensors, coupled with the proper mathematical background, are capable of detecting accelerations and angular velocities and then transforming those into the current position and orientation of the system. A software solution is used to keep track of the orientation of the vehicle and rotate the measurements from the body frame to the navigational frame. Being fully compensated, the IMU is well suited for low accuracy and high dynamic environments, where small size, lightweight and low power consumption demanded. The IMU can provide inertial data up to 400Hz.

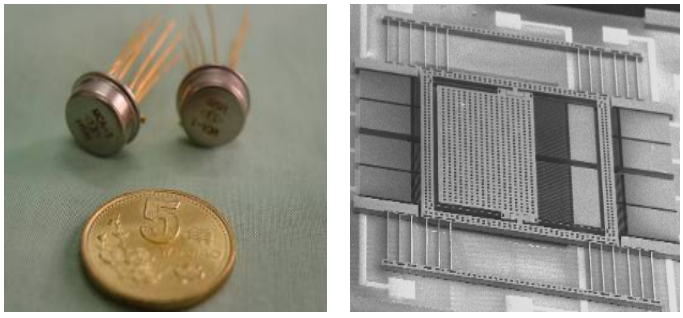

(a) (b)

Fig. 5. MEMS gyro and its microstructure

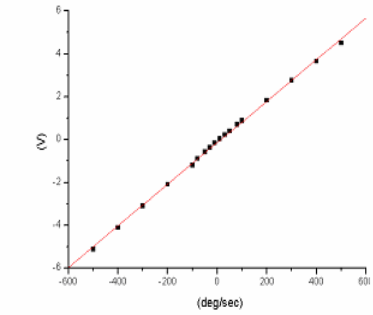

Fig. 6. Gyros response to angular rate

The GPS receiver used in this work is the Fastrax's iTrax02 GPS. The iTrax02 receivers are small size, light weight, ultra low power consumption that have the accuracy less than 6m 95%. They have a navigation sensitivity as low as -150dBm making them applicable even for extremely demanding applications and environments.

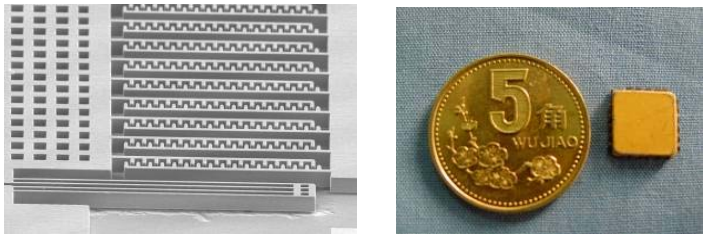

Fig. 7. MEMS accelerometer and its microstructure

The Magnetometer is the Honeywell's HMR3300 electronic compass. The HMR3300 is a three-axis, tilt

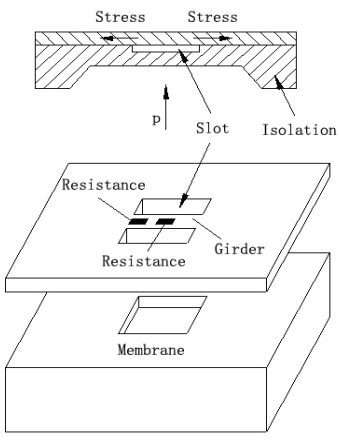

Fig. 8. Structure of MEMS barometer

compensated compass that uses a two-axis accelerometer for enhanced performance up to a ±60º tilt range. At level status, the heading accuracy is 1.0 deg, the roll and pitch accuracy are 0.4 deg.
The barometers used in this work are MEMS barometers developed by our group. Fig. 8 shows the structure of the MEMS barometer. It has an accuracy repeatability with 0.1%FS.

V. Guidance, Navigation and Control loop Introduction

The navigation loop plays a key role in the GNC system. Its navigation outputs are used in guidance and control and affect the performance of the UAV. The core of the navigation loop is the strap-down INS using MEMS inertial sensors and the Kalman filter. The strap-down INS provides reliable position, velocity and attitude with sufficiently high rates. The Kalman filter estimates the navigation errors by blending the GPS observation, baro-altimeter or magnetometer data running as a background task[13,14].

The guidance loop forms an outer control loop in autonomous mode. It computes the guidance demands from the current UAV states and the next way-point information to force the vehicle to follow the desired way-point. The flight control loop forms the inner control loop and it generates the actual control signals to follow the guidance objectives as well as to stabilize the UAV attitude and rate.

A. Strap-down Inertial Navigation System

Fig. 9 shows a block diagram of how a strap-down inertial navigation work[15]. The inertial navigation system is the heart of the navigation sensor system of the UAV. In the last decade, inertial navigation systems using MEMS sensors have been a subject of great interest. The development of MEMS has permitted mass production of devices, though reducing the cost of previously expensive sensors. A strap-down inertial navigation system uses three orthogonal accelerometers and gyros triads mounted to the vehicle to sense the linear and angular motion of the vehicle. The angular motion of the system is continuously measured using the rate sensors. The accelerometers do not remain stable in space, but follow the motion of the vehicle. In this equipment, Navigation is accomplished by a computer using gyro information to resolve the accelerations that are sensed along the carrier axes. This integration of the raw measurements to obtain position and attitude can be done in different coordinate systems. Common are the mechanization in a local level and in a geocentric earth fixed Cartesian coordinate frame.

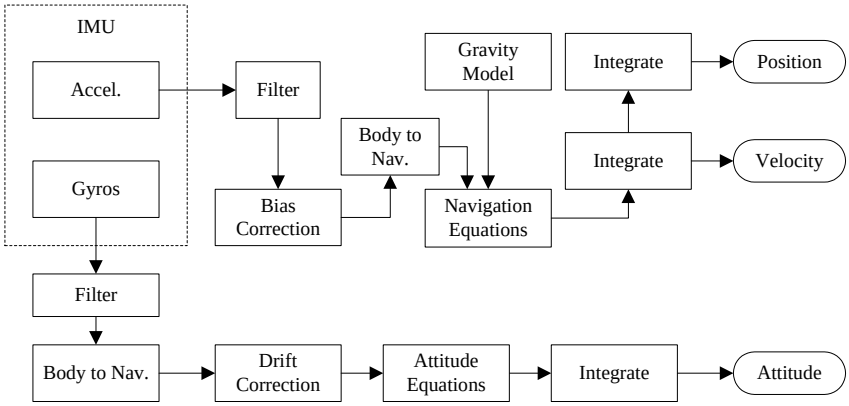

Fig. 9. Flow chart of a strap-down INS

The INS provides high relative accuracy but the absolute accuracy deteriorates with time if the system is running in stand-alone mode and no external update measurements are available. As the INS uses integration techniques to obtain the actual position and attitude, the positioning and attitude

errors grow with time. Most of the error sources that corrupt the navigation solution are sensor errors or random disturbances. The MEMS inertial sensors errors like bias error, scale factor error and random walk noise dominate the INS error growth. These INS errors are typically low dynamics and its models have been well developed[16,17]. Utilizing appropriate external position or velocity update measurements (e.g. provided by GPS observations) the systematic error effects can be mostly eliminated and improved accuracies within the one second interval are theoretically possible. This topic is discussed in the next section of the paper.

B. Fusion Kalman Filter

The Kalman filter is an alternative way of formulating the minimum mean square error filtering problem using state space methods. The fusion Kalman filter is the central part of the integrated navigation system, where the components that are usually used in integration are the INS, GPS, magnetometer and the baro-altimeter. The INS alone has an unavoidable error that grows unbounded as time lapse. The GPS and magnetometer provides the position estimate at relatively slower rate. A Kalman filter was developed to estimate the errors of the system and then update the navigational solution. The purpose of combining navigation subsystems into an integrated system is to take advantage of complementary strengths of the subsystems. Thus the integrated navigation system offers very attractive feature[18,19,20,21]:

(1) The integrated navigation system accuracy improves considerably than that of individual subsystem.

(2) The integrated navigation system has a higher fault-tolerant property because each individual subsystem can still provide (part of) the navigation solution while others are temporarily unavailable because of jamming, GPS signal blockage, or any other reason.

(3) GPS, magnetometer and baro-altimeter may be used for the initialization process of the INS and even for calibration.

Fig. 10 shows the block diagram of the complementary INS/GPS/Baro/Mega Kalman filter that deals with the INS error state instead of the total vehicle states using the INS error model.

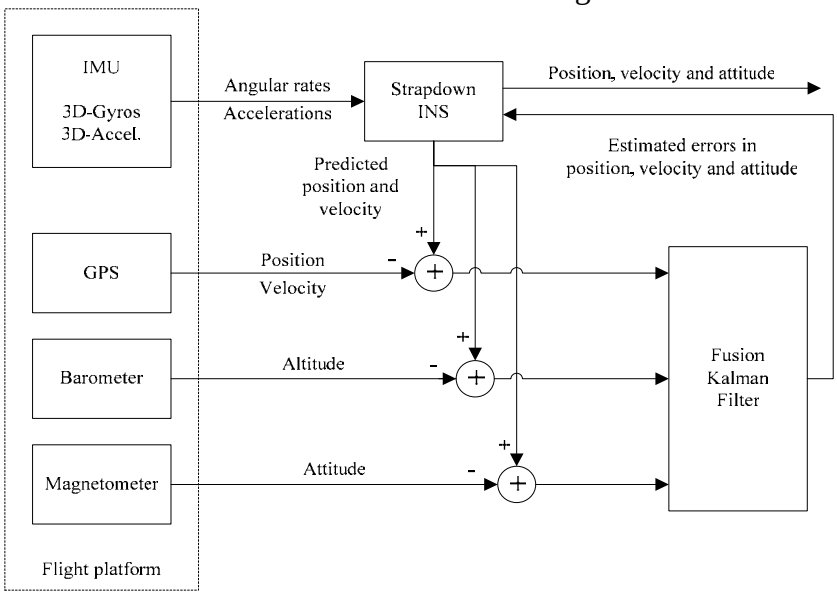

Fig. 10. The structure of INS/GPS/Baro/Mag Kalman filter

C. *Guidance*

The guidance loop computes the guidance demands from the current UAV states and the next waypoint to satisfy mission requirements. The guidance demands are desired UAV airspeed, height and bank angle. In autonomous mode, it selects the appropriate next waypoint depending upon the guidance state. Then it decides if the waypoint has been intercepted or missed. If it is not intercepted, it determines the Line Of Sight (LOS) angles and LOS rates to the next waypoint. Based on this information it computes the lateral acceleration required to intercept the next waypoint and converts this acceleration to the desired bank angle with a set of additional guidance demands: airspeed and height. The guidance loop updates guidance demands every 30Hz.

D. *Flight Control*

The flight control generates servomotor signals for the rudder, elevator, aileron and engine throttle. Using the guidance outputs and measured vehicle states, the flight control performs speed control, height and height rate control, bank angle control, heading control, turn compensation and elevation control. It controls the UAV's attitude, attitude rates and the airspeed. It generates the control signals every 20ms which is limited by the bandwidth of the servomotor. The control loop is the most time critical task in autonomous flight mode. A servomotor is a compact electromechanical device consisting of a DC motor with a built-in feedback circuit. These servomotors accept pulse-width modulation (PWM) signals as the reference input. Fig. 11 shows the block diagram of the control loop[22].

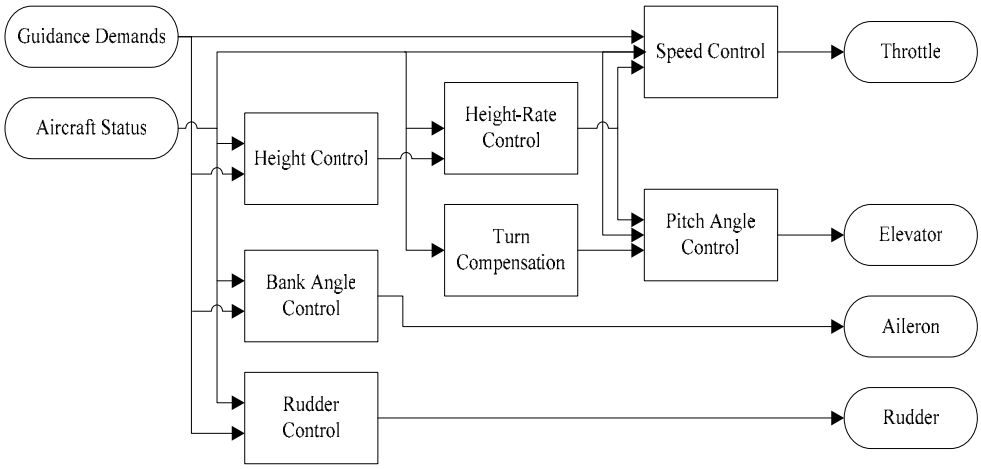

Fig. 11. The control structure

II. Real-Time Results

Due to the limitation of payload capacity of UAV, it is difficult to evaluate the performance of the GNC by adopting a more precise reference system. Instead, the covariance and innovation data from the fusion filter were used to evaluate the performance and the filter consistency. A 30min flight test was performed to verify the real-time autonomous flight with desired waypoint scenario. The desired flight height in autonomous mode was set to 300m above the ground, and the desired air speed was set to 16m/s. Fig. 12 (a), (b), (c) shows the three-axes measured acceleration of the x, y, z-axes accelerometers, respectively. Fig. 13 (a), (b), (c) shows the three-axes measured angular rate of the x, y, z-axes gyroscopes, respectively. Fig. 14 shows the trajectory of the UAV during the activation of autonomous mode. The mean and the maximum of the course-line deviation between GNC estimated position and GPS indicated position are 1.21 and 2.47 meter, respectively.

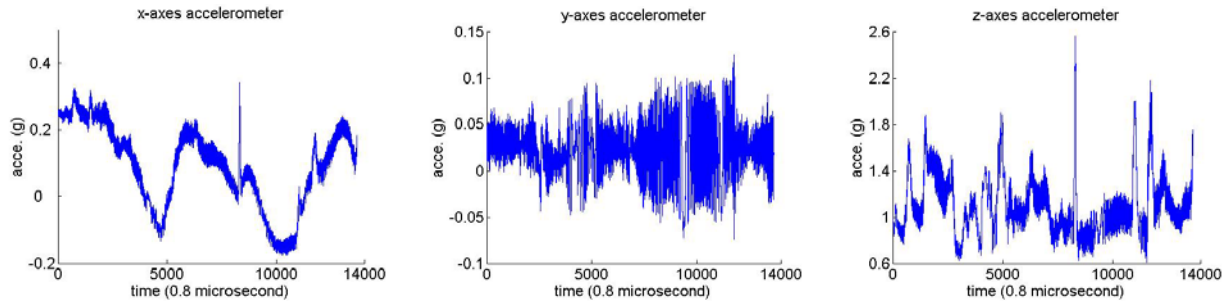

(a) **(b)** **(c)**

Fig. 12. (a) The output of x-axes accelerometer; (b) The output of y-axes accelerometer; (c) The output of z-axes accelerometer.

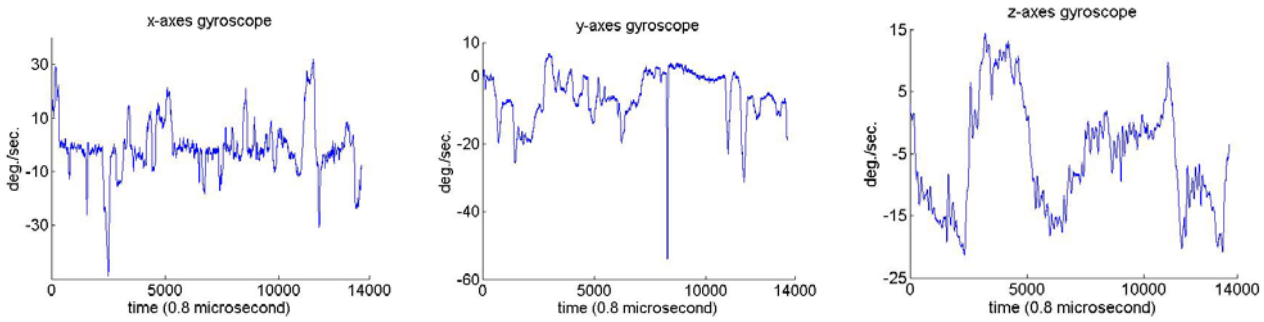

(a) **(b)** **(c)**

Fig. 13. (a) The output of x-axes gyroscope; (b) The output of y-axes gyroscope; (c) The output of z-axes gyroscope.

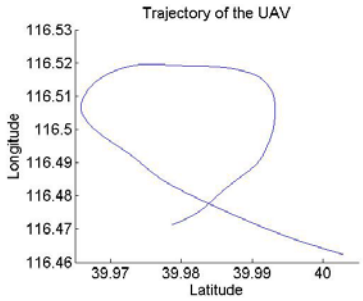

Fig. 14. The trajectory of GNC estimated position.

VI. Conclusions

This paper presents the guidance, navigation, and control of a UAV using MEMS sensors. The MEMS inertial sensors are used for strap-down inertial navigation. A GPS, MEMS baro-altimeter and a magnetometer is uses to estimate and correct the MEMS INS error. The benefits of this integrated system for accurate position, velocity and attitude determination were shown. The air data system provides air pressures. The airspeed can be computed according to the air data. The whole GNC algorithm was implemented in an embedded computer ARM9. The reliable and accurate performances of the GNC are high enough for real-time autonomous flight of UAV.

Acknowledgements

The authors wish to thank Y. J. Yang, who has contributions to MEMS inertial sensors; S. C. Fan, who has contributions to MEMS barometer; and W. J. Wang, who have contributions to the flight platform.

References

[1] H. Shim, *Hierarchical Flight Control System Synthesis for Rotorcraft-based Unmanned Aerial Vehicles*. PhD thesis, Engineering-Mechanical Engineering, University of California, Berkeley, 2000.

[2] F. Ayazi, *The HARPSS Process for Fabrication of Precision MEMS Inertial Sensors*. Mechatronics, vol. 12, pp. 1185-1199, 2002.

[3] B. E. Boser, *Electronics for Micromachined Inertial Sensors*. International Conference on Solid-State Sensors and Actuators, Chicago, June 16-19, IEEE, 1997.

[4] C. C. Painter, *Active Structural Error Suppression in MEMS Vibratory Rate Gyroscope*. IEEE Sensors Journal, vol. 3, No. 5, October 2003.

[5] C. Kevin, etc., *The Design, Fabrication, and Testing of a Micromechanical Silicon Oscillating Accelerometer*. AIAA-98-4399, American Institute of Aeronautics and Astronautics, Inc, 1998.

[6] R. Hulsing, *MEMS Inertial Rate and Acceleration Sensor*. IEEE Aerospace and Electronic Systems Magazine, Vol. 13, Issue 11, 1998.

[7] A. Warnasch, A. Killen, *Low Cost, High G, High Accuracy, Micro Electro-Mechanical Systems (MEMS) Inertial Measurements Unit (IMU) Program*. Position Location and Navigation Symposium, IEEE, 15-18 April, 2002, pp. 299-305.

[8] D. Cardarelli, *An Integrated MEMS Inertial Measurement Unit*. Position Location and Navigation Symposium, IEEE, 15-18 April, 2002, pp. 314-319.

[9] F. X. Cao, etc., *Low Cost SINS/GPS Integration for Land Vehicle Navigation*. The IEEE 5th International Conference on Intelligent Transportation Systems 3-6, September 2002, Singapore.

[10] A. K. Brown, *Test Results of a GPS/Inertial Navigation System Using a Low Cost MEMS IMU*. Proceedings of 11th Annual Saint Petersburg International Conference on Integrated Navigation System, Saint Petersburg, Russia, May 2004.

[11] S. Sukkarieh, E. M. Nebot, and H. F. Durrant-Whyte, *A High Integrity IMU/GPS Navigation Loop for Autonomous Land Vehicle Applications*. IEEE Transactions on Robotics and Automation, Vol. 15, No. 3, June 1999.

[12] J. Zhang, Z. Jin, and W. Tian, *A Suboptimal Kalman Filter with Fading Factors for DGPS/MEMS-IMU/Magnetic Compass Integrated Navigation*. Proceedings of Intelligent Transportation Systems, Vol. 2, 12-15 Oct. 2003, IEEE, pp. 1229-1234.

[13] A. Seigert, *An Alternative Formulation for the Integration of GPS and INS Measurements*. http://www.nav.uni-stuttgart.de/navigation/publikationen/2003/seifert_isprs.pdf.

[14] A. Brown, D. Sullivan, *Precision Kinematic Alignment Using a Low-Cost GPS/INS System*. Proceedings of ION GPS 2002, Portland, Oregon, September 2002.

[15] P. G. Savage, *Strapdown Inertial Navigation Integration Algorithm Desogn Part I: Attitude Algorithms*. Journal of Dynamic Systems, Measurement and Control, Vol. 21(1), pp. 19-28, 1998.

[16] K. J. Walchko, etc., *Embedded Low Cost Inertial Navigation System*. Florida Conference on Recent Advances in Robotics, FAU, Dania Beach, FL, 2003.

[17] D. G. Meskin, I. Y. Bar-Itzhack, *Unified Approach to Inertial Navigation System Error Modeling*. Journal of Guidance, Control, and Dynamics, Vol. 15(3), pp. 648-653, 1992.

[18] S. Sukkarieh, *Aided Inertial Navigation systems for Autonomous Land Vehicles*. PhD thesis, Australian Centre for Field Robotics, The University of Sydney, 1999.

[19] J.H. Kim, *Real-time Navigation, Guidance, and Control of a UAV using Low-cost Sensors*. http://www.acfr.usyd.edu.au/publications/downloads/2003/Kim197/FSR03-NavGuidCtrl-Kim, 2003.

[20] A. B. Chatfield, *Fundamentals of High Accuracy Inertial Navigation (Progress in Astronautics and Aeronautics) (Hardcover)*. Published by AIAA, 1997, ISBN:156347230.

[21] R. M. Rogers, J. A. Schetz, *Applied Mathematics in Integrated Navigation System*. AIAA Education Series, Hardcover, Published by AIAA, 2000.

[22] R. Brown, P. Hwang, *Introduction to Random Signals and Applied Kalman Filtering*. Third Ed., John Wiley and Sons, 1997.

Z. J. Huang was born in QingTao, China, in 1968. He received his PhD from Beijing University of Aeronautics and Astronautics in 1992. He is now a post-doctor in school of Instrumentation Science & Optoelectronics Engineering of Beijing University of Aeronautics and Astronautics. His current research interests include guidance, navigation and control, image matching, multisensor image registration, and multisensor image fusion.

J. C. Fang was born in 1965 and received BS, MS and PhD from Shandong University of Technology, Xi'an Jiaotong University and Southeast University in 1983, 1988, 1996 respectively. Now he is professor and dean of Instrumentation Science & Optoelectronics Engineering of Beijing University of Aeronautics and Astronautics. His research interests include navigation, guidance and control of aerocraft, information fusion of multi sensor in addition to precision machine system and autocontrol theory.